Powder Technology 400 (2022) 117256

Contents lists available at ScienceDirect

Powder Technology

journal homepage: www.elsevier.com/locate/powtec

Fabric effect on the angle of repose in granular materials

Bei-Bing Dai [a,b,*], Tian-Qi Li [a], Lin-Jie Deng [a], Jun Yang [c], Wei-Hai Yuan [d]

[a] School of Civil Engineering, Sun Yat-sen University, Guangzhou, China
[b] Southern Marine Science and Engineering Guangdong Laboratory (Zhuhai), Zhuhai, China
[c] Department of Civil Engineering, The University of Hong Kong, Hong Kong, China
[d] College of Mechanics and Materials, Hohai University, Nanjing, China

ARTICLE INFO

Article history:
Received 6 October 2021
Received in revised form 24 February 2022
Accepted 1 March 2022
Available online 5 March 2022

Keywords:
Granular heap
Angle of repose
Fabric anisotropy
Deposition
Discrete element method

ABSTRACT

In the present study, we perform a series of physical model experiments and numerical simulations to examine the effect of fabric orientation on angle of repose. The results show that with the deposition plane orientation angle θ varying from 0° to 90°, the angle of repose α reduces firstly and then rebounds, and the minimum values emerge at $\theta = 30° \sim 45°$. Numerical analyses indicate that the microstructure reorganization becomes more intense as θ varies from 0° to 90°, making the anisotropy magnitude decrease and the principal anisotropy direction transit to a specific direction. With the analysis based on a conceptual model, we make a clarification on the fundamentals underlying the effect of fabric orientation on the angle of repose α. By introducing a θ-dependent coefficient, we propose an expression of α as a function of principal anisotropy directions (ϕ_n and ϕ_p) of the contact and particle orientations.

1. Introduction

"Heap" is a characteristic presence pattern of powders and bulk solids (i.e. particulate or granular materials), which is widespread in nature and frequently encountered in our daily life [1–3]. Granular heaps (piles) are generated by the accumulation of a great number of particles under the effect of gravity or other external effects such as wind blow and water flow, and this accumulation process is also interpreted as the heaping (piling) of discrete particles. The maximum slope angle for granular heaps is referred to as "angle of repose", which is thought to be one of the most important parameters characterizing the physical and mechanical properties of granular materials. Angle of repose is extensively applied for various purposes in the scientific and industrial fields which involve dealing with granular materials (e.g., geography, geology, agriculture, food engineering, civil engineering, chemical engineering, pharmaceutical engineering, etc.). The local "pressure dip" at the bottom of a granular heap is a fascinating phenomenon as well, which has long been observed in the experiments and reproduced in the numerical simulations [4–14]. It is obviously of fundamental importance to understand the mechanical properties associated with granular heaps such as angle of repose and pressure dip.

Over the past several decades, researchers have devoted considerable efforts, through either experimental or numerical approaches, to examining the formation of granular heaps and exploring the related fundamentals. Zhou et al. [15] carried out both experiments and numerical simulations to investigate the influence of various factors, including the basic particle attributes, on the macroscopic features of granular heaps, and found that the angle of repose rises as the inter-particle sliding or rolling coefficient increases, and reduces with the increasing particle size. The numerical simulations done by Matuttis [11] revealed that the particle size distribution plays a vital part in the macroscopic properties of granular heaps, and that increasing the polydispersity of composing particles contributes to the increase of angle of repose and also helps strengthen the local pressure dip underneath granular heaps. Goldenberg and Goldhirsch [8] reproduced through numerical simulations, the local bottom pressure dip under the apex of a granular heap, and found that this phenomenon becomes more apparent if the inter-particle friction coefficient is getting small. Using molecular dynamics simulation, Lee and Herrmann [16] and Maleki et al. [17] also came to realize that the angle of repose increases with the increases of inter-particle friction coefficient, which is congruous to the findings from the DEM simulations conducted by Zhou et al. [15] and McDowell et al. [18]. By focusing on the effect of particle shape, Robinson and Friedman [19] performed the physical model tests with the alleged Hele-Shaw cells and achieved the finding that the angle of repose promotes as the circularity of outer particle surface decreases. The works of other researchers (e.g. Dai et al. [20,21], Chen et al. [22], Alonso et al. [23], Zhao et al. [24] and Zhou et al. [25]) have also evidenced that the more irregular the particle shape is, the higher the angle of repose is. It is observed by Zhu et al. [26] that the local pressure dip at the

* Corresponding author at: School of Civil Engineering, Sun Yat-sen University, Guangzhou, China.
E-mail address: daibb@mail.sysu.edu.cn (B.-B. Dai).

https://doi.org/10.1016/j.powtec.2022.117256
0032-5910/

bottom of a granular heap tends to be more conspicuous at a larger particle aspect ratio.

Interestingly, researchers have also brought forward several theoretical models to gain a fundamental understanding of angle of repose [23,27,28]. Alonso et al. [23] developed on the basis of a simple lattice model, an analytical expression of angle of repose as a function of various microscopic factors such as particle shape and surface roughness. Carstensen and Chan [27] established a mathematical relationship between particle size and angle of repose for powders. Similarly, through extensive DEM simulations, Elekes and Parteli [28] proposed a theoretical expression of angle of repose by incorporating the factors of particle size as well as gravity. The previous studies obviously suggest that there exists a strong correlation between macroscopic characteristics of granular heaps and basic particle properties.

Furthermore, the construction history has been identified to be an important factor affecting the formation of granular heaps, as well as their macroscopic attributes. Vanel et al. [5] constructed in the experiments, the granular heaps by the "point-source release method", which refers to an approach of releasing particles from a point source, and observed an obvious pressure dip at the heap bottom. However, granular heaps which were constructed by the "rainfall release method" failed to demonstrate the phenomenon of pressure dip. The rainfall release method means that particles are dropped from an area source, the covering area of which is not less than the bottom area of final granular heaps. Similarly, the molecular dynamics simulations of Matuttis [11] and Matuttis et al. [12] indicate that the angle of repose of granular heap built by the rainfall release method or in the layered sequence is higher than that for the heap constructed by the point-source release method. It is revealed by the photoelastic experiments of Geng et al. [29] that the heaps generated by the point-source release method tend to show the pressure dip, while those made by releasing particles from a source with a relatively large width, do not display the pressure dip at the bottom, and such observations have been confirmed by the DEM simulations of Horabik et al. [30] and Zhou and Ooi [31]. From previous studies, it is therefore reasonable to come to the conclusion that the construction history exerts a significant impact upon the formation of granular heaps, as well as their basic characteristics such as angle of repose and bottom pressure dip. It should be pointed out that the influence of construction history, in essence, results from the fabric created during the construction process. It can be thus said that fabric plays a crucial part in the macroscopic properties of granular heaps.

It is noticed that in previous studies, researchers commonly built granular heaps with the memory of construction history by various particle release methods (e.g., point source, line source, area source, sources of varying width or height, etc.), and scrutinized the influence of construction history (i.e. fabrics or grain-scale structures) on the macroscopic characteristics of heaps (e.g., angle of repose and bottom stress distribution). Few works have been done till now to associate the macro features of granular heaps such as angle of repose with the fabric. In present study, we perform the physical model tests and numerical simulations, in which we construct granular heaps with the rainfall release method which, however, is practiced in a manner different from that reported in the literature. The orientation angle of deposition plane relative to the horizontal plane is varied from 0° to 90° degrees, which helps produce fabrics with various orientations, such that we investigate the influence of fabric orientations on the characteristics of granular heaps. For the convenience of experimental practice in creating fabrics having various orientations, an apparatus with a rotatable container is developed for containing particles deposited under gravity at various container tilting angles (i.e. at different deposition plane orientation angles), so that we are able to obtain granular heaps with various fabric orientations. In this study, a comparison analysis on angles of repose is made between the experiments and numerical simulations; by virtue of the DEM simulations, we analyze the fabric anisotropy in granular heaps, and explore its linkage with the angle of repose from both qualitative and quantitative perspectives. It is hoped that we can gain from this study, an in-depth understanding into the role played by the fabric in the formation of granular heaps and the related macroscopic features.

2. Experimental and numerical implementation

2.1. Experimental implementation

We develop an experimental apparatus as shown in Fig. 1, which includes the container box, bottom base, rotatable shaft, gap at the corner for discharging redundant particles, to perform the granular heap tests with focus on the effect of fabric. With the aid of a jack, the container box can be rotated freely around the rotatable shaft. The dimensions of container box are $l \times h \times b = 1020\ \text{mm} \times 1020\ \text{mm} \times 40\ \text{mm}$. Note that this apparatus is different from a rotatable drum. This is because the rotatable container used in the current study can only have a limited rotation and is for the examination of the angle of repose for granular

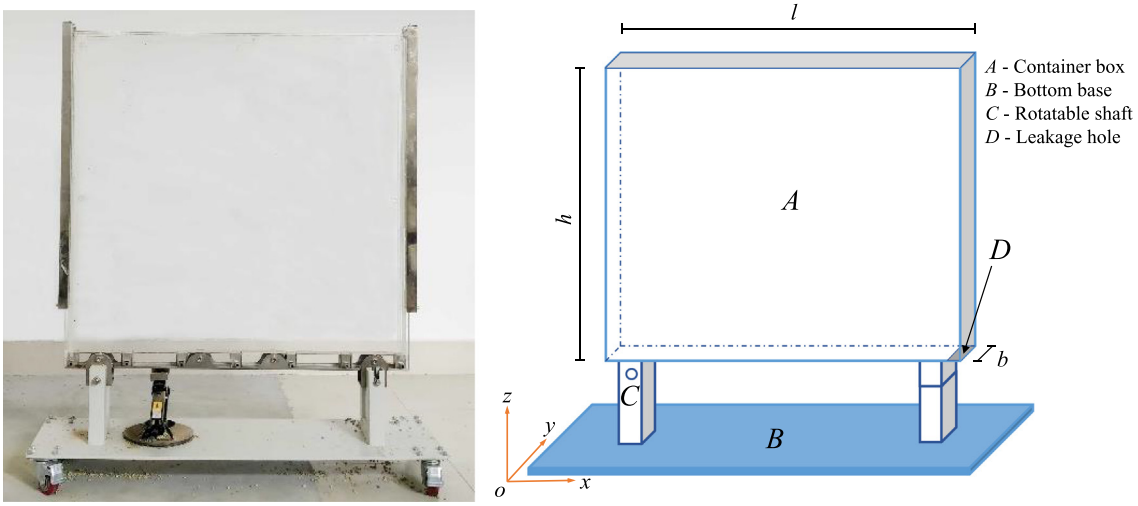

Fig. 1. The apparatus developed for testing: (a) the real object; (b) schematic description of apparatus.

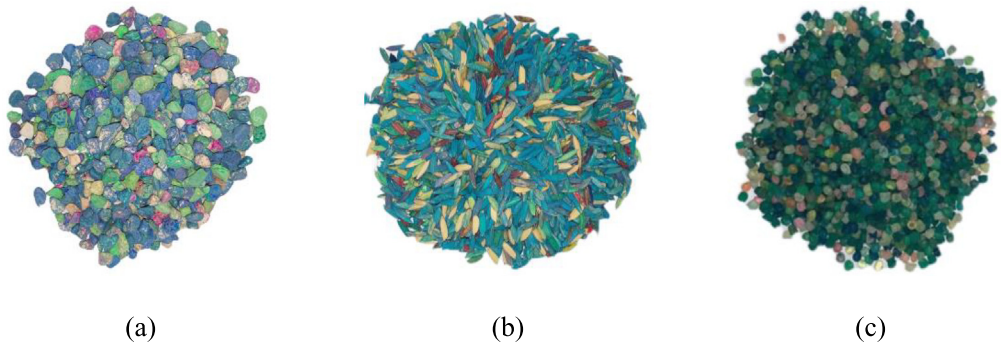

Fig. 2. Granular materials used in the experiment: (a) diatomite particles; (b) rice grains; (c) PVC particles.

materials in a static packing state, but a rotatable drum can enjoy a persistent rotation and is mainly used to study the convection and segregation of granular materials in motion, as well as the dynamic angle of repose. As shown in Fig. 2, three materials are used, and they are made up of the diatomite particles, rice grains and polyvinyl chloride (PVC) particles, respectively. Table 1 gives the basic attributes for the three materials.

To build a granular heap with a particular fabric orientation, we firstly employ a jack to stabilize the container box at a certain tilting angle θ, as shown in Fig. 3a. Subsequently, we desiccate the material used and deposit the particles layer by layer by releasing them in a manner of rainfall, as depicted in Fig. 3b. It is worth noting that for a better visualization of layered structures, we dyed the particles in two neighboring layers with two different colors, to produce the pattern of visually alternating layers, whereas the material constituent is all the same for various layers. The container tilting angle θ (i.e. the orientation angle of deposition plane) considered includes $\theta = 0°$, 15°, 30°, 45°, 60°, 75° and 90°. Upon the completion of particle deposition process, we carefully rotate the container box, together with the deposited granular mass, back to the normal position (i.e. the box bottom being horizontal and the lateral wall being vertical), as indicated in Fig. 3c, such that the granular mass is expected to have a particular fabric orientation. We then discharge the surplus particles through the corner gap until a stable granular heap is generated without any particle flows (see Fig. 3d), and we measure the angle of repose α; that is, we do the measurement of angle of repose after the avalanche of superficial particles on the top of the stable granular heap. Note that at a given orientation angle θ, we repeat the tests five times to obtain five heaps, and thus we have five α values for a specific θ angle.

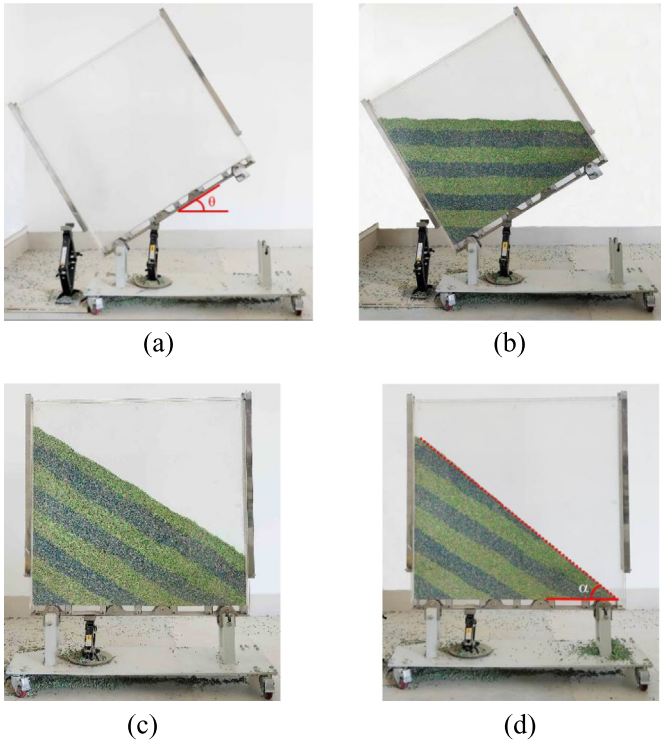

Fig. 3. The experimental procedure for the rainfall release method: (a) stabilization of the container at a tilting angle θ; (b) deposition of particles; (c) restoration to the normal position; (d) final granular heap.

2.2. Numerical implementation

We use the DEM program PFC3D to simulate the granular heap construction in the experiments. The particles in the numerical model, as shown in the inset in Fig. 4a, are composed of two spheres which are clumped with each other, and the two children spheres cannot be torn apart. The aspect ratio of a particle is given by the length ratio between the minor and major axes [32–35] and the value is specified to be 0.556 in this study. It should be noted that we here focus on a study of the effect of fabric on the angle of repose, and thus we use an idealized elongated particle shape in the DEM simulation for the isolation of the effect of particle shape. It is well accepted that the particle shape in reality is rather complex, and researchers have devoted many efforts to exploring the linkage between particle shape and macroscopic bulk behaviors of granular systems [36–38]. In particular, the effect of particle shape may be coupled with the effect of fabric. For instance, the deposition of elongated particles tends to give a more anisotropic fabric as compared with rounded particles. This is the reason why we employ an idealized elongated grain shape in the DEM simulations in this study, which helps produce anisotropic microstructures and facilitates the examination of the fabric effect on the angle of repose.

Table 1
Parameters for granular materials.

Granular materials	Aspect ratio	Bulk density (g/cm^3)	Major axis (mm)	Intermediate axis (mm)	Minor axis (mm)
Diatomite particles	0.53	0.427	8.05–11	5.11–7.99	3.98–6.71
Rice grains	0.39	0.582	8–9.99	3.02–3.93	2.98–3.76
PVC particles	0.57	0.593	4.95–5.99	3.06–3.02	2.86–3.42

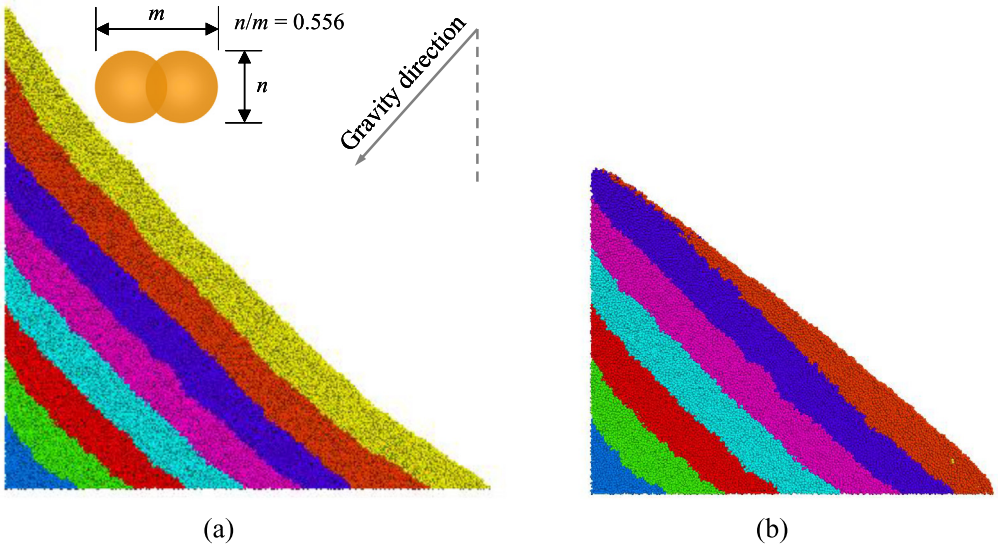

Fig. 4. Construction of a granular heap ($\theta = 45°$) in numerical simulations: (a) particle deposition completed; (b) final granular heap.

The particle density is 2.65 g/cm^3. The particle sizes (in diameter) range between 1.7 cm and 1.9 cm. For the reduction of scale effect and the ease of particle deposition, the dimensions of container box are adopted to be $l \times h \times b$ = 2000 mm × 2000 mm × 160 mm. The particle-wall stiffness in both normal and tangential directions is set to be 1.0×10^5 N/m. The contact behavior between particles is governed by a linear elastic model. The particle-particle stiffness in the normal and tangential directions is 1.0×10^5 N/m as well. The contact friction behavior obeys the Coulomb friction law and the friction coefficient is given to be 0.5 for both particles and walls. The damping ratio is 0.5.

Owing to that the gravity direction can be adjusted in the DEM simulation, we create the fabric with various orientations by depositing particles under the effect of gravity (g = 9.8 m/s^2) at different directions; that is, we do not rotate the container box in the numerical simulation. Take the numerical case with the gravity direction at θ = 45° as an example. Fig. 4a presents the numerical model after the layer-by-layer deposition of particles, and the layer thickness is controlled to be around 200 mm. When the deposition is finished, the gravity is restored to a normal state, with its direction reset to be in the vertical downward direction. Fig. 4b shows the eventual granular heap after the discharge of redundant particles under the effect of gravity in the vertical downward direction. The number of particles in such a numerical model is around 5×10^4. With the numerical model in Fig. 4b, we can perform the measurement of angle of repose and the fabric analysis. Note that an important index, namely, mratio (i.e., the ratio of the maximum unbalanced force against the mean value of the contact force, applied force and body force magnitudes over all bodies), is employed in PFC3D to ensure the equilibrium state for the final granular heap, and the reference value is set to be 1.0×10^{-3} in this study. If the mratio value is less than or equal to 1.0×10^{-3}, a granular heap is considered to have arrived at an equilibrium state; otherwise, additional cycling is needed to meet the mratio requirement.

3. Micromechanical index and anisotropy characterization

The fabric of a granular assembly is usually referred to as the spatial arrangement of the particles and contacts in this assembly. For a quantitative description of fabric, a number of vectors such as the particle and contact orientation vectors are proposed to characterize the microstructures in an assembly, and employed to formulate the alleged "fabric tensor" [39–44]. Take the contact orientation vector for example. For each contact between two particles, we define a pair of unit vectors, which are normal to the contact plane and possess opposite directions. This pair of unit vectors are called as "contact unit normal vectors". Suppose there are N contacts within an assembly. There will be in total 2 N contact unit normal vectors, and a fabric tensor is formulated through an averaging procedure as [39].

$$F_{ijlm\cdots} = \frac{1}{2N}\sum_{k=1}^{2N} n_i^k n_j^k n_l^k n_m^k \cdots \tag{1}$$

where n_i^k (i = 1, 2, 3 for a 3D case, and i = 1, 2 for a 2D case) are the direction cosines of a contact unit normal vector n^k with respect to the reference axes X_i (i = 1, 2, 3, and i = 1, 2 for a 2D case) in a Cartesian coordinate system. $F_{ijlm\cdots}$ can be rewritten as a second-ranked tensor for simplification.

$$F_{ij} = \frac{1}{2N}\sum_{k=1}^{2N} n_i^k n_j^k \tag{2}$$

In addition, a density function $E(n)$ is introduced to characterize the spatial distribution of unit vectors over the representative elemental volume (REV), such that the fabric tensor in Eq. (2) is re-expressed in the integral form [40].

$$F_{ij} = \int_{\Omega} E(n) n_i n_j \mathrm{d}\Omega \tag{3}$$

where Ω denotes the REV, and the density function $E(n)$ is given as.

$$E(n) = E_0(1 + d_{ij} n_i n_j) \tag{4}$$

where E_0 refers to the distribution probability density of unit vectors at an isotropic state and equals $1/(2\pi)$ for a 2D case; d_{ij} is a second-ranked deviatoric tensor characterizing the deviation from an isotropic distribution. $E(n)$ in Eq. (4) for a 2D case is a periodic function with a period of 2π. With the substitution of n_i and n_j with the direction cosines, Eq. (4) can be further derived to be.

$$E(\phi) = E_0(1 + d_{11}\cos 2\phi + d_{12}\sin 2\phi) \tag{5a}$$

$$E(\phi) = E_0\left\{1 + \sqrt{d_{11}^2 + d_{12}^2}\left(\frac{d_{11}}{\sqrt{d_{11}^2 + d_{12}^2}}\cos 2\phi + \frac{d_{12}}{\sqrt{d_{11}^2 + d_{12}^2}}\sin 2\phi\right)\right\} \tag{5b}$$

where ϕ refers to an interested direction. Rothenburg and Bathurst [40] alternatively used the following expression for the density function

$$E(\phi) = E_0\{1 + a_n \cos 2(\phi - \phi_n)\} \tag{6}$$

where a_n and ϕ_n are two important indices characterizing the fabric anisotropy relating to the contact unit normal vector, with a_n giving the magnitude of anisotropy and ϕ_n defining the principal direction of anisotropy, and they are expressed as.

$$a_n = \sqrt{d_{11}^2 + d_{12}^2} \text{ and } \phi_n = \frac{1}{2}\arctan\left(\frac{d_{12}}{d_{11}}\right) \tag{7}$$

The value of $E(\phi)$ in Eq. (6) gives the distribution probability density of contact unit normal vectors at a specified direction ϕ. Rothenburg and Bathurst [40] put forward as well other continuous functions similar to Eq. (6), to describe the angular distributions of other essential vectors characterizing the microstructures and contact force network in an assembly, and the functions for the particle orientation unit vector and contact normal force vector are given to be

$$P(\phi) = E_0\left\{1 + a_p \cos 2\left(\phi - \phi_p\right)\right\} \tag{8}$$

$$f(\phi) = f_0\left\{1 + a_f \cos 2\left(\phi - \phi_f\right)\right\} \tag{9}$$

where f_0 is the measure of mean contact normal force with the contacts in different directions given equal weight; a_p and a_f represent the anisotropy magnitudes of the particle orientation unit and contact normal force vectors; ϕ_p and ϕ_f denote the principal directions of anisotropy.

In the experiments and numerical simulations, particles are released through a line source, with the deposition plane oriented (or equivalently oriented) at an angle varying from 0° to 90° degrees. In this context, the anisotropy associated with the distribution of internal structures and contact force network in a granular heap is supposed to develop principally in the plane where particles precipitate; that is, the fabric and force anisotropy, as indicated by the coordinate system in Fig. 1b, exists primarily in the plane of *xoz*. Hence the anisotropy analysis in terms of the microstructures and contact force network in granular heaps centers on their distributions in the particle precipitation plane. To this end, all vectors concerned here are projected onto this plane for a statistical analysis of anisotropy.

4. Results and analyses

4.1. Observed angle of repose in granular heaps

Fig. 5 describes the relations between the observed angle of repose α and the orientation angle of deposition plane θ for granular heaps in the experiments and numerical simulations. It is found that α does not show a monotonically increasing or decreasing trend with the variation of θ, and it suffers from an interim dip at the range of $\theta = 30° \sim 45°$, irrespective of which material is used in the test. The relation of angle of repose with θ in the numerical simulations also shows good agreement with the experimental observation. That is, with the increase of θ from 0° to 90°, the angle of repose α decreases at first, with the minimum value taking place at $\theta = 30° \sim 45°$, and then undergoes a rebound with the further increase of θ. The minimum α values for PVC particles and rice grains, which emerge at $\theta = 30°$, are 40.13° and 42.34°, respectively, and for diatomite particles, the minimum value of α is 40.06° when $\theta = 45°$. The minimum angle of repose in the numerical simulations occurs at $\theta = 30°$, and the value is 39.1°. In addition, the angles of repose for rice grains are in general higher than those for the PVC and diatomite particles, and the angles of repose for the latter two materials are a little bit close to each other. This is probably because rice grains possess more irregular particle shapes as compared with the PVC and diatomite particles, as indicated in Fig. 2.

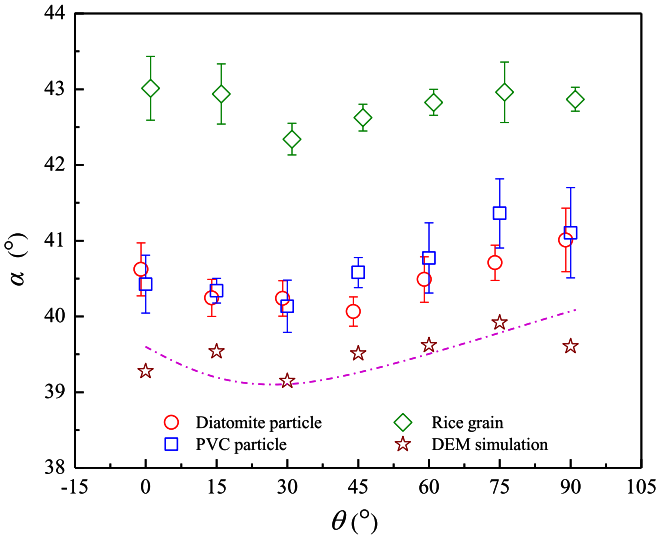

Fig. 5. The relations of angle of repose α with the orientation angle θ of deposition plane.

It is also interesting to note that the angles of repose given by the numerical simulations are in general smaller than those obtained from the tests, and this is presumably ascribed to the use of idealized numerical model of granular heap in the DEM simulations. The detailed reasons include but are not limited to: firstly, the idealized particle shape in the numerical model may not capture the shape complexity in the real sense; secondly, the particle-scale contact model used is a linear elastic contact model which may fail to completely characterize the true inter-particle contact behavior; thirdly, the particle rolling resistance is not taken into account in the DEM simulations.

4.2. Observed fabric and force anisotropy in granular heaps

(a) Contact orientations

Fig. 6 describes the variations of the fabric anisotropy indices of a_n and ϕ_n relating to contact orientations, with the deposition plane orientation angle θ. It is observed that the anisotropy magnitude a_n before the avalanche of redundant granular masses (i.e. before the formation of granular heap), which is obtained by a statistic analysis with focus on the zone corresponding to the profile of final granular

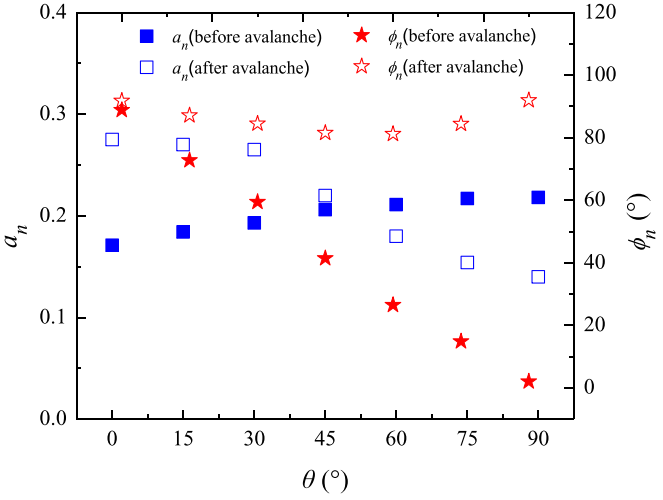

Fig. 6. The relations of fabric anisotropy indices a_n and ϕ_n with the orientation angle θ of deposition plane.

heap, is basically around 0.2, despite that it exhibits a weak increasing trend as θ varies from 0° to 90°. The principal anisotropy direction ϕ_n prior to the avalanche of granular masses, decreasing from 88.82° to 1.95° when θ increases from 0° to 90°, is almost perpendicular to the deposition plane orientation direction (θ). After the removal of surplus granular masses under the effect of gravity in the vertical downward direction, the anisotropy magnitude a_n with respect to the distribution of contact unit normal vectors in the eventual granular heaps, is seen to decrease with the variation of θ from 0° to 90°, and ϕ_n, as indicated in Fig. 6, is around 90° (i.e. near the vertical direction). However, we are still able to find that the principal anisotropy direction (ϕ_n) of contact unit normal vectors in the final granular heaps suffers from a temporary minor drop within the range of $\theta = 45° \sim 75°$; that is, it firstly reduces and then rebounds as θ varies from 0° to 90°.

It is interesting to note from the data in Fig. 6 and the rose diagrams in Fig. 7 that the anisotropy magnitude a_n after avalanche is enhanced at $\theta = 0°$, with the principal anisotropy direction ϕ_n being almost unchanged. This is probably ascribed to that the reorganization of microstructures during the avalanche of redundant particles induces a "strengthening" effect on the fabric anisotropy of contact orientations in case that the principal anisotropy direction is coincident with the direction of gravity field. It is also seen from the contour maps of fabric anisotropy indices in Fig. 8 that a_n is increased in the zone near the slope surface of granular heap, and ϕ_n within the granular heap, which is on the average close to 90°, does not change dramatically after avalanche. In the low θ region ($\theta < 45°$), with the increase of θ the angle deviation between the vertical direction of gravity field and the principal anisotropy direction before avalanche escalates, which leads to increasingly intense microstructure reorganizations and reduction of "strengthening" effect on the fabric anisotropy during avalanche. As a result, the anisotropy magnitude a_n after avalanche reduces with θ ($< 45°$), but it is still higher than the value prior to avalanche. In the meantime, the principal anisotropy direction ϕ_n adjusts through the microstructure reorganization, to the vertical direction (90°). Despite this, it seems to become more difficult for the microstructure reorganization to take place if the principal anisotropy direction before avalanche increasingly deviates from the vertical gravity direction as θ increases. Therefore ϕ_n after avalanche shows a slight reduction with θ, with the increase of the gap between ϕ_n and the vertical direction (90°).

As θ continues to increase, the angle deviation between the vertical gravity direction and the principal anisotropy direction before avalanche gets larger and larger, which brings about more and more intense microstructure reorganizations upon the avalanche of surplus granular masses under the effect of gravity. Interestingly, the angle deviation is so large at a high θ angle that the intense microstructure reorganizations may even cause a "crushing" effect, rendering a sharp transition of the principal anisotropy direction. It is clear that ϕ_n at $\theta = 90°$ transits from about 0° (before avalanche) to about 90° (after avalanche) as indicated by the data in Fig. 6 and the rose diagrams in Fig. 7. In this connection, the anisotropy magnitude a_n keeps decreasing when θ varies from 45° to 90°, and the principal direction of anisotropy ϕ_n undergoes a minor increase beyond the range of $\theta = 45° \sim 75°$.

The contour maps in Figs. 8-10 show that the distributions of the anisotropy indices of a_n and ϕ_n before avalanche are, to some extent, in a uniform pattern. In the avalanche process of redundant granular masses, the microstructure reorganizations have substantially affected the original uniform distribution of fabric anisotropy. It is observed that the zone near the slope surface is subject to the most severe influence, in which ϕ_n is almost in the vertical direction and the anisotropy magnitude a_n is relatively large as compared with the values in other regions. This is because this zone is exposed to the disturbance of granular flows generated by the avalanche of redundant particles in the upper part under the effect of gravity. Note that the unit of the coordinates in all contour maps is meter.

(b) Particle orientations

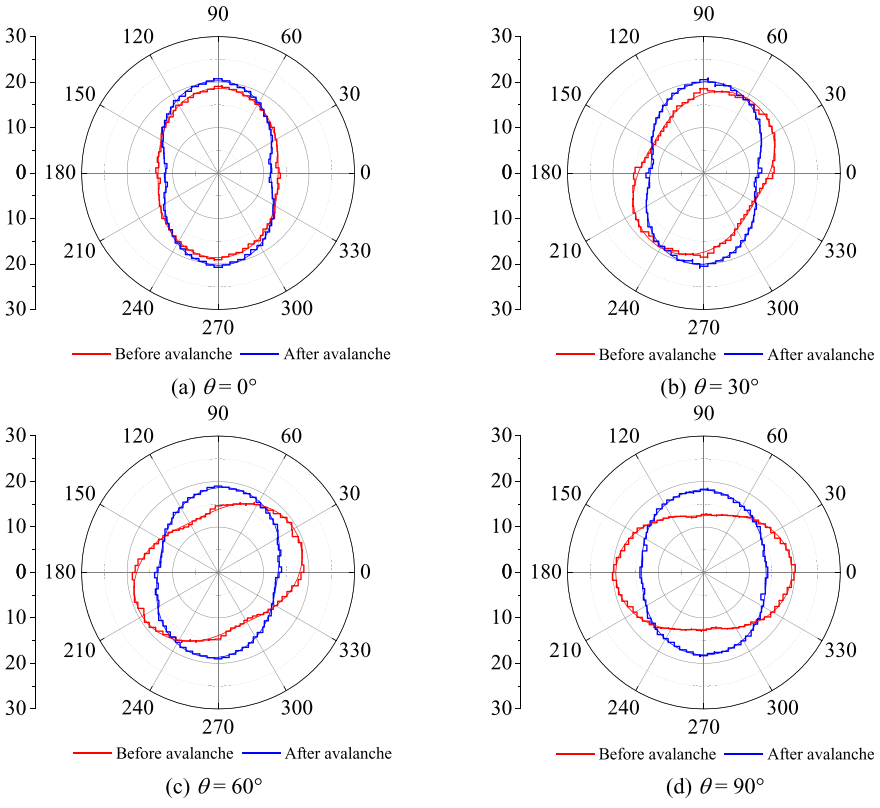

Fig. 7. Comparison of angular distribution probability densities (%) of contact unit normal vectors at the states prior to and after the avalanche of redundant particles.

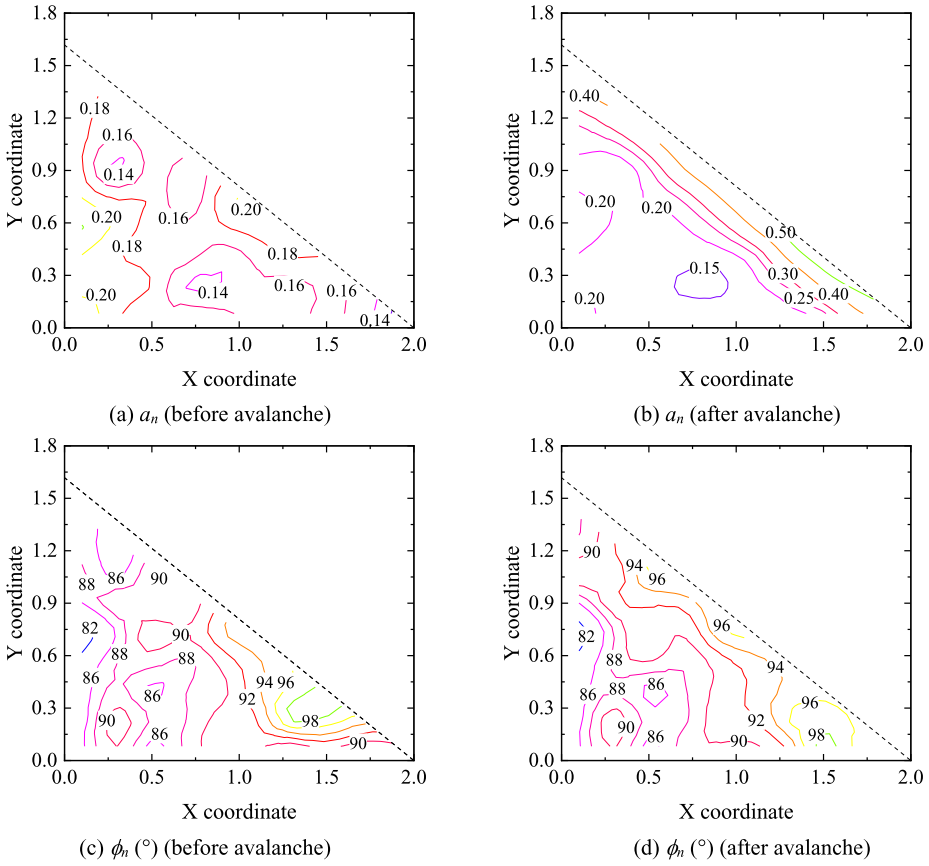

Fig. 8. Comparison of contour maps for the distribution of fabric anisotropy associated with contact orientations at the states prior to and after the formation of granular heap ($\theta = 0°$).

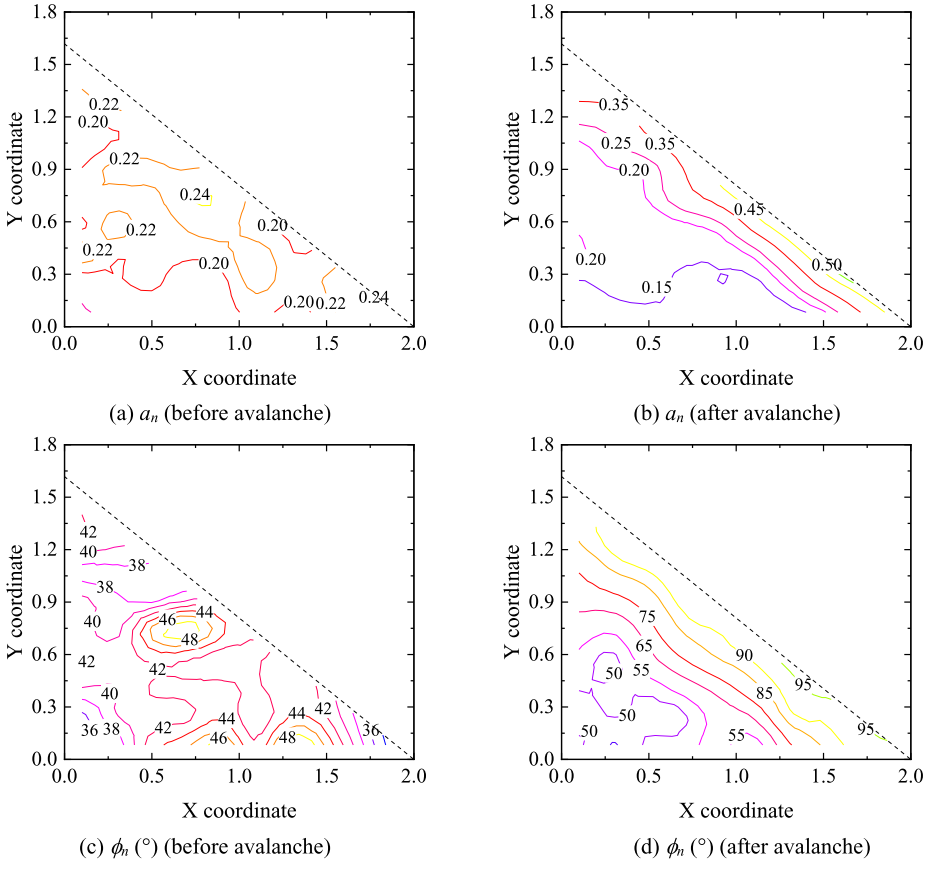

Fig. 9. Comparison of contour maps for the distribution of fabric anisotropy associated with contact orientations at the states prior to and after the formation of granular heap ($\theta = 45°$).

Fig. 11 shows the relations between the fabric anisotropy characterized by particle orientation unit vectors and the deposition plane orientation angle θ, by focusing on the granular heaps constructed through particle avalanching, as well as the corresponding zone of granular heaps in the deposited granular masses before avalanche. It is seen that the anisotropy magnitude a_p before the avalanche of superficial granular masses above the top surface of granular heap, exhibits a decreasing tendency against the angle θ, and meanwhile the principal direction of anisotropy ϕ_p evolves from about 180° (the horizontal direction) to about 90° (the vertical direction) as θ varies from 0° to 90°, with ϕ_p and θ being basically supplementary to each other. The anisotropy magnitudes after the avalanche of redundant particles are seen not to differ considerably from the values before avalanche, and the principal anisotropy direction also does not change significantly in the low θ ($< 45°$) region, while it displays remarkable differentiations in the high θ ($\geq 45°$) region. In particular, it is interesting to note that there also exists a temporary drop in ϕ_p around $\theta = 75°$.

At $\theta = 0°$, it seems that the microstructure reorganization fails to contribute to an obvious alleged "strengthening" effect, since both the anisotropy magnitude a_p and principal direction of anisotropy ϕ_p, as indicated by Figs. 11 and 12, do not differ distinctly from those before avalanche, meaning that the microstructure reorganization does not proceed in a fierce manner. In fact, when θ is lower than 45°, the microstructure reorganization in terms of particle orientations is not that intense to induce noteworthy variations in both a_p and ϕ_p (see Figs. 11 and 12). When θ is above 45°, increasing θ appears to lead to more intense microstructure reorganizations in respect of particle orientations, which are manifested by the notable transitions of principal anisotropy directions. Nevertheless, the anisotropy magnitude a_p is seen not to alter markedly. The minor increase of ϕ_p after the interim dip at $\theta = 75°$ suggests a kind of "crushing" effect caused by the intense microstructure reorganizations, which give rise to a significant transition in the principal anisotropy direction. It is inferred that the reorganization of microstructures relating to particle orientations is not as intense as that for contact orientations, in that the latter is involved with the variation of both anisotropy magnitude and principal anisotropy direction, but the former exerts a distinct impact merely on the principal direction of anisotropy.

Figs. 13-15 present the contour maps describing the distribution of fabric anisotropy of particle orientations in granular heaps. It is obvious that the fabric anisotropy distributions, similar to the observations from Figs. 8-10, are more or less in a uniform fashion. Upon the avalanche of redundant particles during the construction of granular heaps, the microstructure reorganizations have contributed to a nonuniform distribution of fabric anisotropy. Also, the zone near the slope surface is most seriously influenced by the disturbance of granular flows in the avalanche process, with ϕ_p being nearby the horizontal direction and a_p being relatively large in this zone.

(c) Contact normal force

Fig. 16 presents the variations of the force anisotropy indices a_f and ϕ_f before and after avalanche, with the orientation angle θ of deposition plane. It is seen that the relations of a_f and ϕ_f with θ are somewhat analogous to those observed in Fig. 6 for the indices of a_n and ϕ_n. With θ varying from 0° to 90°, the anisotropy magnitude a_f prior to avalanche is at an approximately constant level (around 0.3), and the principal direction of anisotropy ϕ_f transits from about 90° (the vertical direction) to about 0° (the horizontal direction). Given the state after the avalanche of redundant granular masses, the anisotropy magnitude a_f exhibits a monotonic decrease from about 0.3 at $\theta = 0°$ to about 0.07 at $\theta = 90°$, and the principal anisotropy direction ϕ_f is beside the vertical direction (90°), with a temporary drop occurring at $\theta = 45° \sim 75°$.

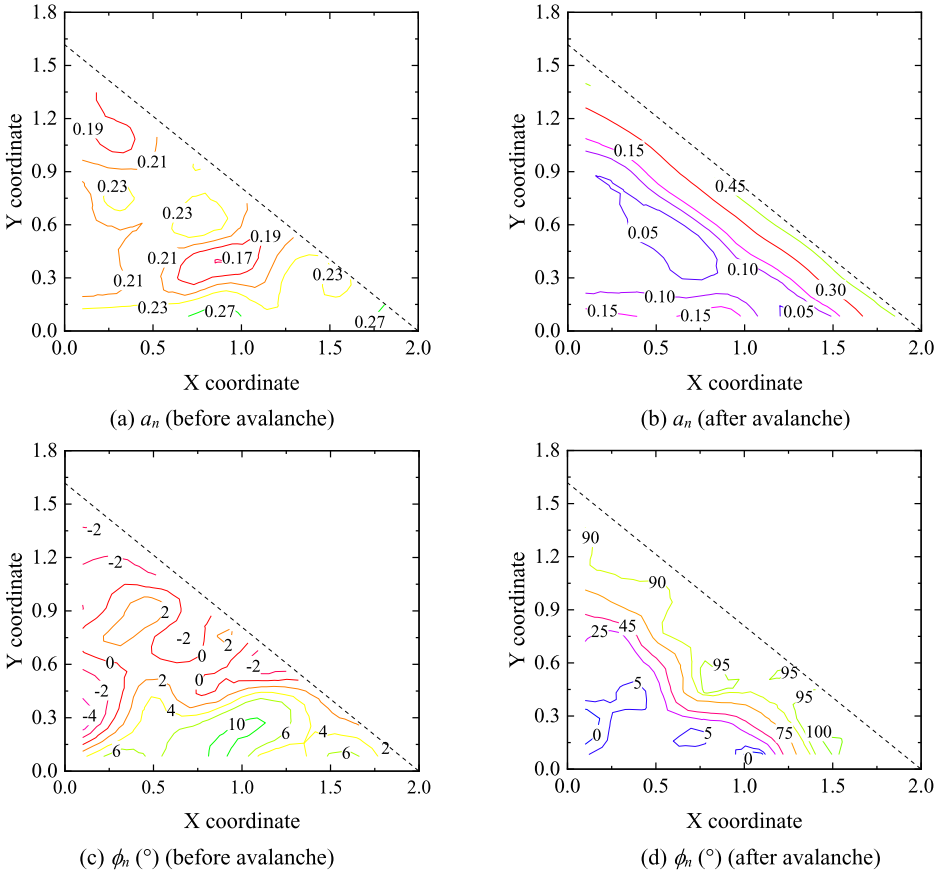

Fig. 10. Comparison of contour maps for the distribution of fabric anisotropy associated with contact orientations at the states prior to and after the formation of granular heap ($\theta = 90°$).

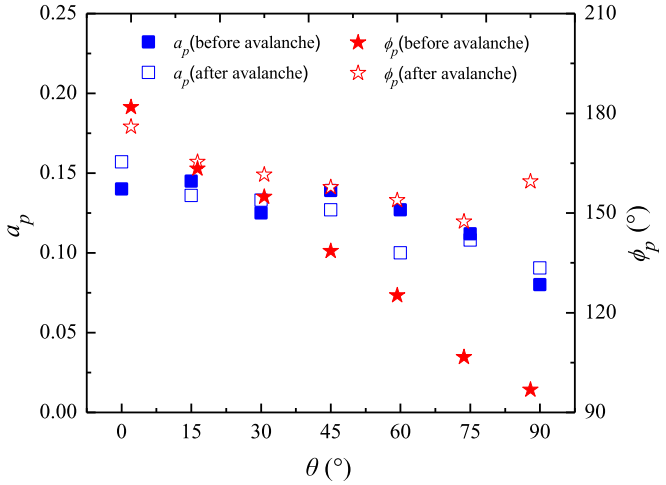

Fig. 11. The relations of fabric anisotropy indices a_p and ϕ_p with the orientation angle θ of deposition plane.

In general, if the principal direction of anisotropy ϕ_f before avalanche coincides with or approximates to the vertical gravity direction, the distribution anisotropy of contact normal forces, as evidenced by the values of a_f and ϕ_f at $\theta = 0°$ in Fig. 16 and the rose diagrams in Fig. 17, will be less affected by the microstructure reorganizations during the avalanche of redundant particles, and a_f has in fact slightly decreased. With θ increasing from 0° to 90°, the escalation of the angle deviation between the principal anisotropy direction (before avalanche) and the vertical gravity direction tends to lead to more intense microstructure reorganizations, making a_f (after avalanche) reduce and ϕ_f adjust to the vertical direction (see Figs. 16 and 17). The slight decreasing trend of ϕ_f in the low θ region is due probably to that it is a little more difficult for the reorganization of microstructures to take place at a relatively large angle deviation, and this will in turn make the transition of principal direction of force anisotropy more difficult. However, if the angle deviation between the principal anisotropy direction (before avalanche) and the vertical gravity direction is adequately large, the alleged "crushing" effect associated with intense microstructure reorganizations, is expected, which is responsible for a minor increase of ϕ_f beyond the range of $\theta = 45° \sim 75°$.

In addition to the variations of the force anisotropy (i.e. the anisotropy magnitude a_f and principal anisotropy direction ϕ_f) amid the formation process of granular heaps, the overall force magnitude decreases as well. As observed from the angular distributions of average contact normal forces in Fig. 17, the maximum force magnitude has decreased from a value around 1.5 N to a value around 1.0 N, owing to the removal of granular masses above the final granular heap. The absence of the alleged "strengthening" effect on the force anisotropy magnitude, which, in fact, suffers from a minor decrease at a given low θ value, may be linked with the unloading effect resulting from the removal of redundant granular masses. Figs. 18-20 show the contour maps characterizing the distribution of force anisotropy. The distributions prior to avalanche are also seen to be in an almost uniform pattern, and the distributions after avalanche are influenced by the involved microstructure reorganizations during the avalanche process. The zone right underneath the slope surface of granular heap is mostly affected as the anisotropy magnitudes are higher than those in other regions and the principal anisotropy directions are next to the vertical direction.

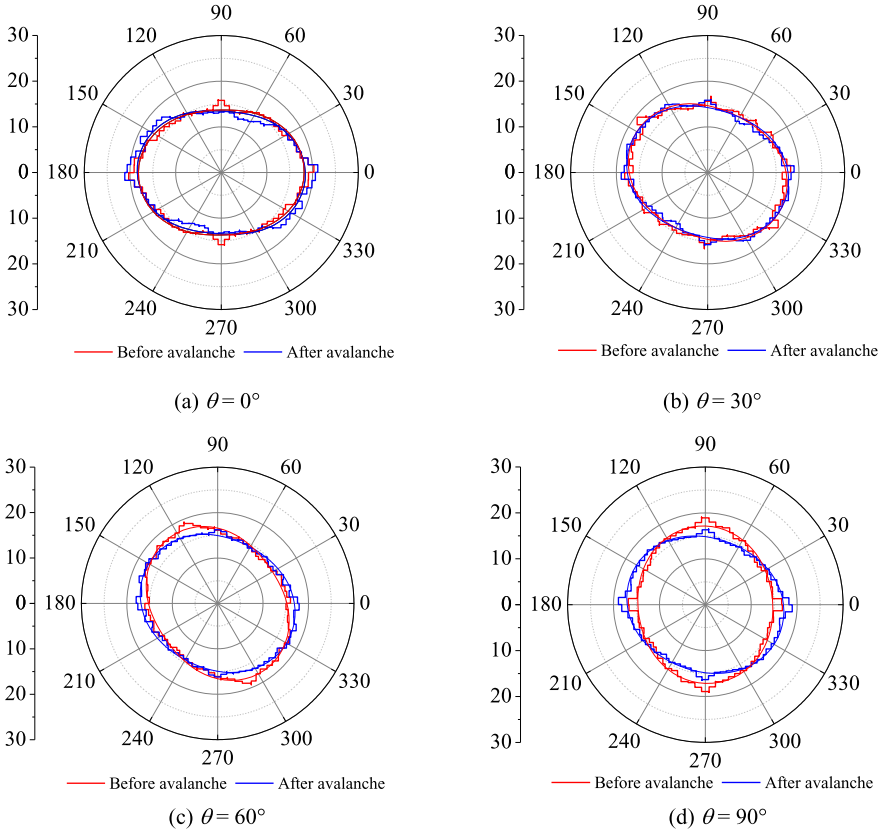

Fig. 12. Comparison of angular distribution probability densities (%) of particle orientation unit vectors at the states prior to and after the avalanche of redundant particles.

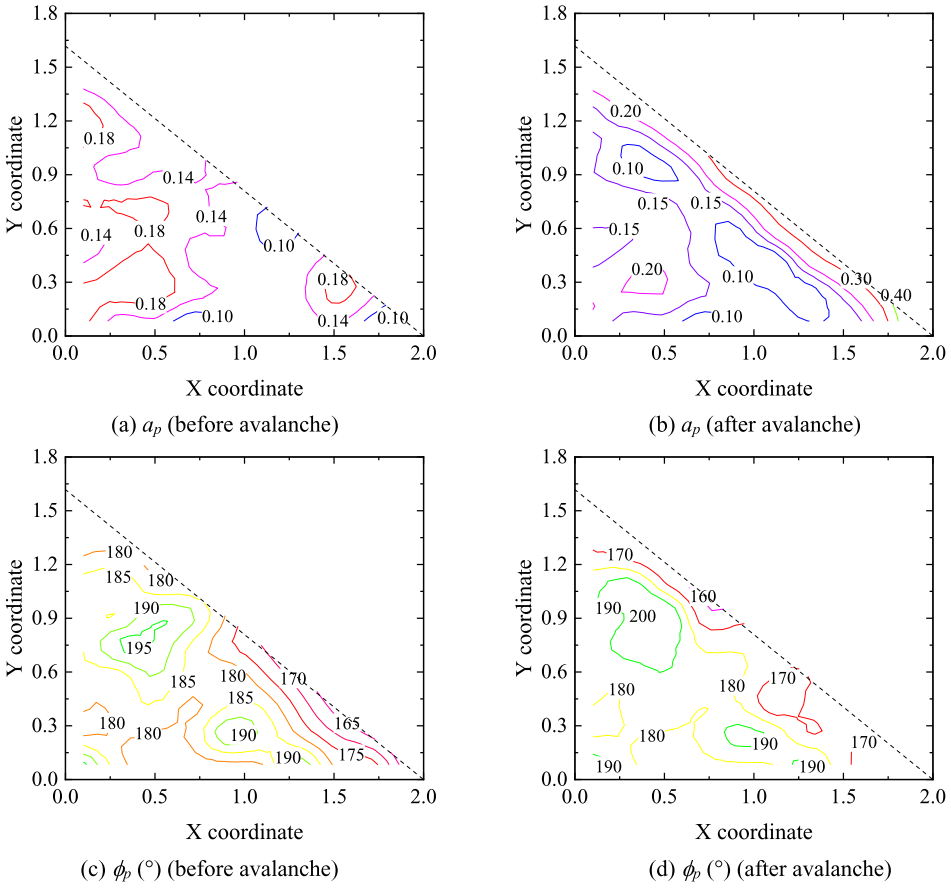

Fig. 13. Comparison of contour maps for the distribution of fabric anisotropy associated with particle orientations at the states prior to and after the formation of granular heap ($\theta = 0°$).

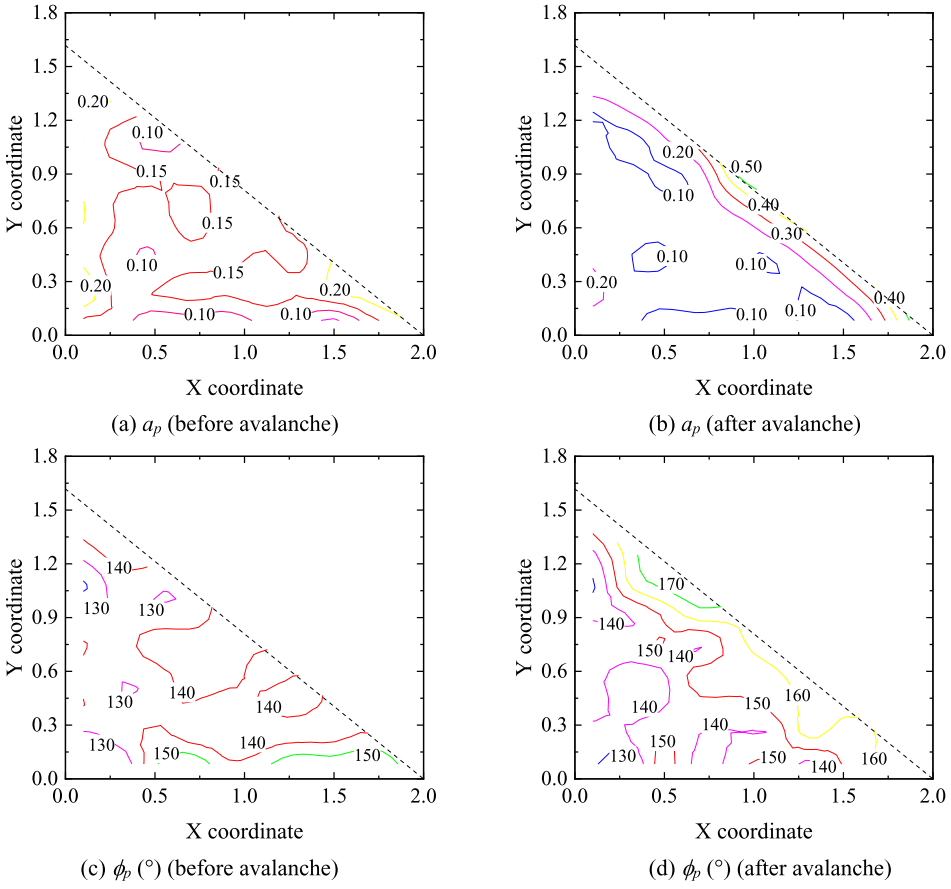

Fig. 14. Comparison of contour maps for the distribution of fabric anisotropy associated with particle orientations at the states prior to and after the formation of granular heap ($\theta = 45°$).

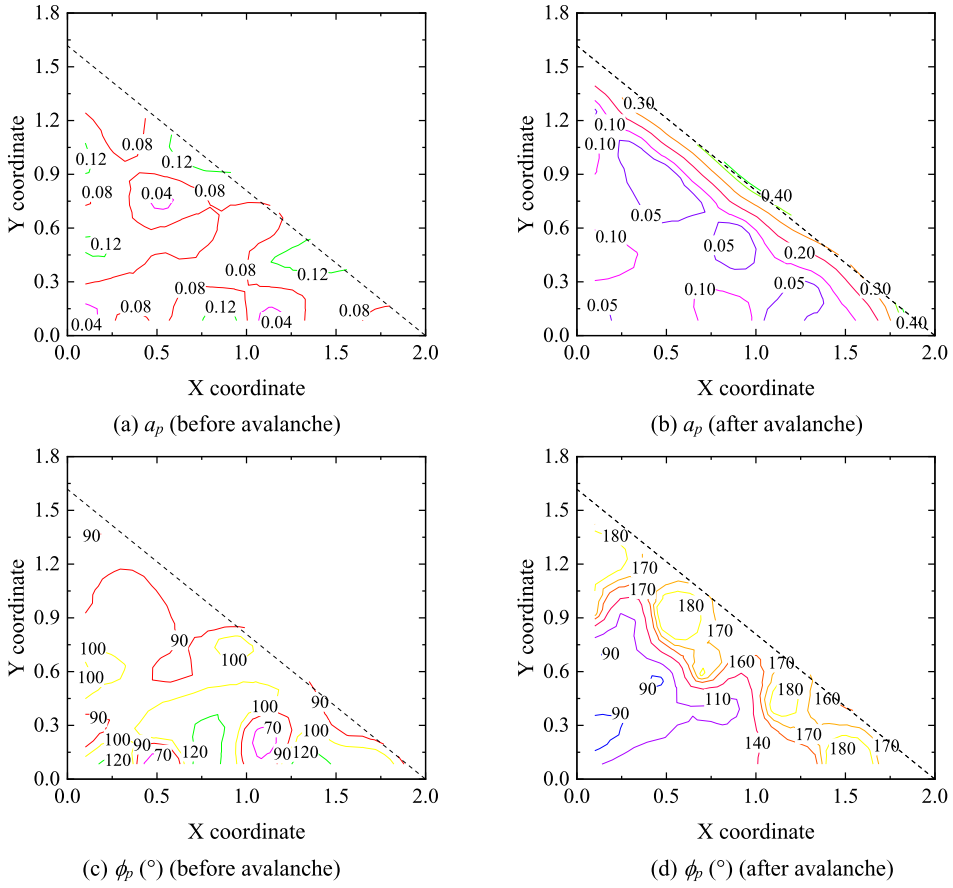

Fig. 15. Comparison of contour maps for the distribution of fabric anisotropy associated with particle orientations at the states prior to and after the formation of granular heap ($\theta = 90°$).

5. Discussion

5.1. Explanation on the effect of deposition plane orientation angle on angle of repose

The literature [15,25,45–49] shows that the angle of repose for granular materials which are commonly encountered in the daily life, generally falls in a typical range of 25° ~ 50°. The measured values of angle of repose in this experimental and numerical study are apparently within this range. It is easy to find from Fig. 5 that the angle of repose is the smallest when θ is within the traditional range of angle of repose; that is, the angle of repose tends to be the smallest when θ (= 30° ~ 45°) is close to the slope angle of granular heap, and the more θ deviates from the traditional range, the greater the angle of repose is.

As indicated in Fig. 21a, the formation of a granular heap through the avalanche of redundant granular materials can be regarded as a kind of sliding shear failure under the self weight of avalanche part. In case that the dynamic effect during the sliding shear process is neglected, the downward force from the avalanche part, as a component of its self weight along the sliding plane (i.e., the potential slope surface), is in balance with the upward sliding friction force, and this equilibrium relation is expressed as

$$mg \sin \alpha = \mu mg \cos \alpha \tag{10}$$

where α is the slope angle of granular heap (i.e., angle of repose), μ is the sliding friction coefficient along the sliding plane. μ is in fact related to the shear strength of granular materials and expressed as $\mu = \tan \phi$, wherein ϕ is the friction angle characterizing the shear strength. Thus Eq. (10) is transformed into

$$\mu = \tan \phi = \tan \alpha \tag{11}$$

The equation above suggests that angle of repose is a manifestation of shear strength of granular materials, and α is to some extent equivalent to ϕ. Therefore, in terms of the relationship between α and θ, the statement in the texts above can be restated as.

"The closer the orientation of deposition plane is to the potential sliding failure plane (i.e., the potential slope surface of granular heap), the smaller the angle of repose is, and the more the deposition plane orientation deviates from the potential sliding failure plane, the larger the

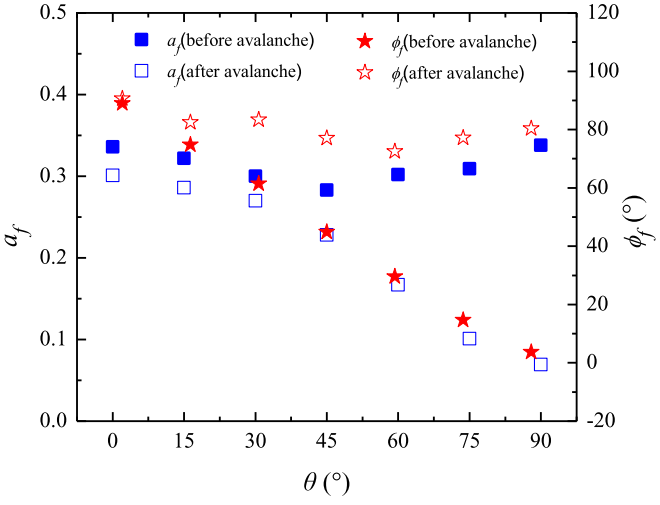

Fig. 16. The relations of force anisotropy indices a_f and ϕ_f with the orientation angle θ of deposition plane.

angle of repose is. It can be also said that the more the deposition plane orientation approximates to the potential shear failure plane, the smaller the friction angle (i.e., shear strength) is, and the more the orientation of deposition plane deviates, the higher the friction angle is."

As a matter of fact, a number of researchers have investigated the effect of orientation angle of deposition plane on the shear strength of granular soils, and found that when the orientation of deposition plane is close or parallel to that of the potential shear failure plane, the shear strength is the lowest. For instance, Fu and Dafalias [50] did a numerical simulation of biaxial compression test, as shown in Fig. 21b, and revealed that when δ, the angle formed between the deposition plane and the shear failure plane, is 0°, the shear strength reaches a minimum value. Miura et al. [51] conducted the hollow cylinder torsion shear experiments and also validated that the minimum shear strength is achieved when the deposition plane is parallel to the potential sliding plane. Cao et al. [52] developed a strength criterion for the transversely isotropic sandy soil, and made with it a prediction that if the deposition plane is oriented around $45° + \phi/2$, i.e., the deposition plane is almost parallel to the shear failure plane, the shear strength will be the smallest. Such studies have in fact tacitly proved that the closer the orientation of deposition plane is to the potential sliding failure plane, the smaller the angle of repose will be, and the more the deposition plane orientation deviates, the larger the angle of repose will be.

Zuriguel and Mullin [53] performed a photo-elastic test of sandpile formation and observed that when particles are deposited under the effect of gravity, their orientations are mostly distributed nearby the deposition plane, and this has also been verified in the current DEM simulations. As described in Fig. 22a, if the orientation of deposition plane is close to the potential sliding failure plane, particle orientations tend to be parallel to the sliding failure plane, such that the interlocking effect between particles along the potential sliding failure plane is supposed not to be that strong. As a consequence, particles need to do less work to overcome the resistances in the sliding process, and it is comparatively easy for the granular mass to arrive at a lower-energy state, contributing to a relatively small angle of repose. Note that less work required to overcome the resistances in the sliding process means lower shear strength mobilized during the sliding failure of avalanching granular mass. However, if the deposition plane orientation, as seen in Fig. 22b, deviates considerably from the potential sliding plane, most particle orientations deviate from the potential sliding plane, leading to a more marked interlocking effect between particles. In this connection, there needs to be more work done to overcome the resistances, and it is not easy for granular mass to avalanche and reach a state of low energy. Thus a relatively large angle of repose is desired. It is also worth pointing out that more work needed to overcome the resistances denotes higher mobilized shear strength for the sliding granular mass.

The illustrations above have clarified the reason why α is prone to have a minimum value in case that the orientation ($\theta = 30° \sim 45°$) of deposition plane is close to the potential sliding failure plane (i.e., the potential slope surface of granular heap). It should be noted that the orientation of potential sliding failure plane lies in the typical range of 25° ~ 50°.

5.2. Correlation of angle of repose with fabric anisotropy

We note from the experimental and numerical results that the angle of repose is dependent on the particle deposition direction, the variation of which helps create the fabric having various preferred orientations in granular heaps. It is thus natural to establish a link between the angle of

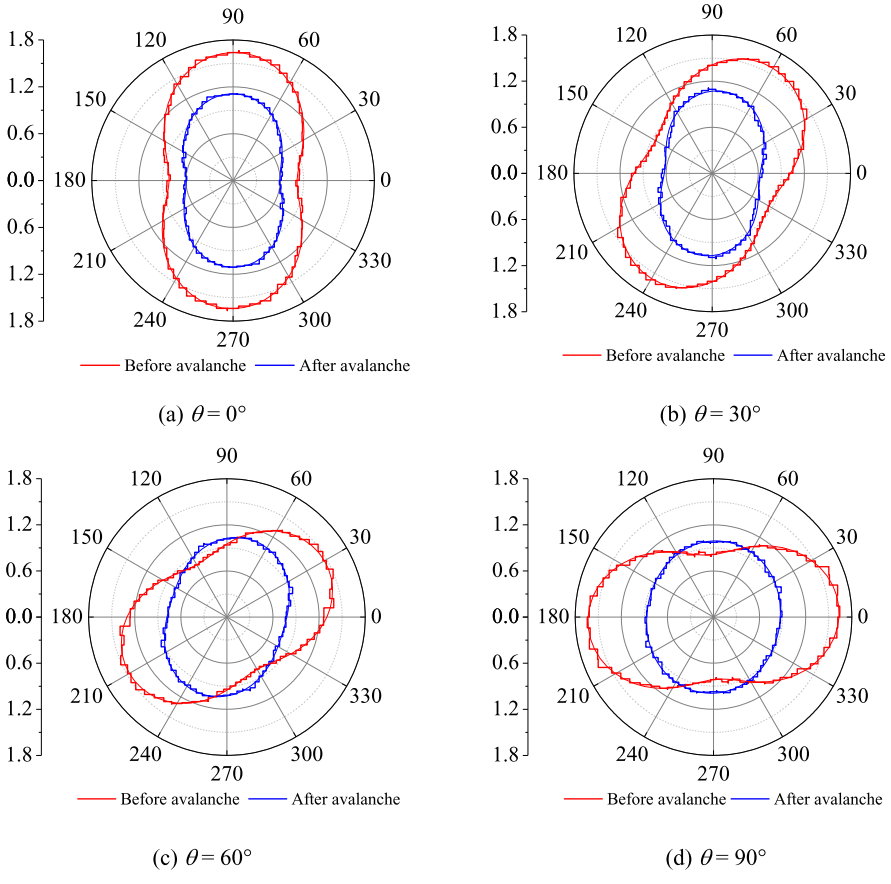

Fig. 17. Comparison of angular distributions of mean contact normal forces (N) at the states prior to and after the avalanche of redundant particles.

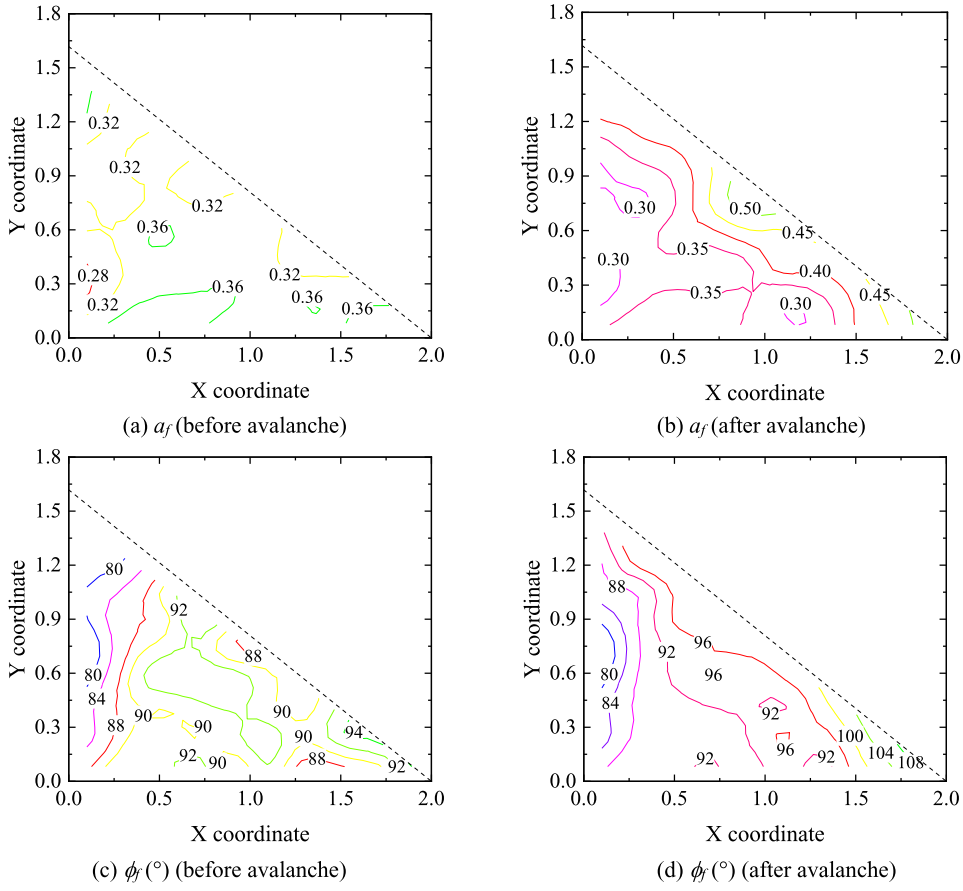

Fig. 18. Comparison of contour maps for the distribution of force anisotropy associated with contact normal forces at the states prior to and after the formation of granular heap ($\theta = 0°$).

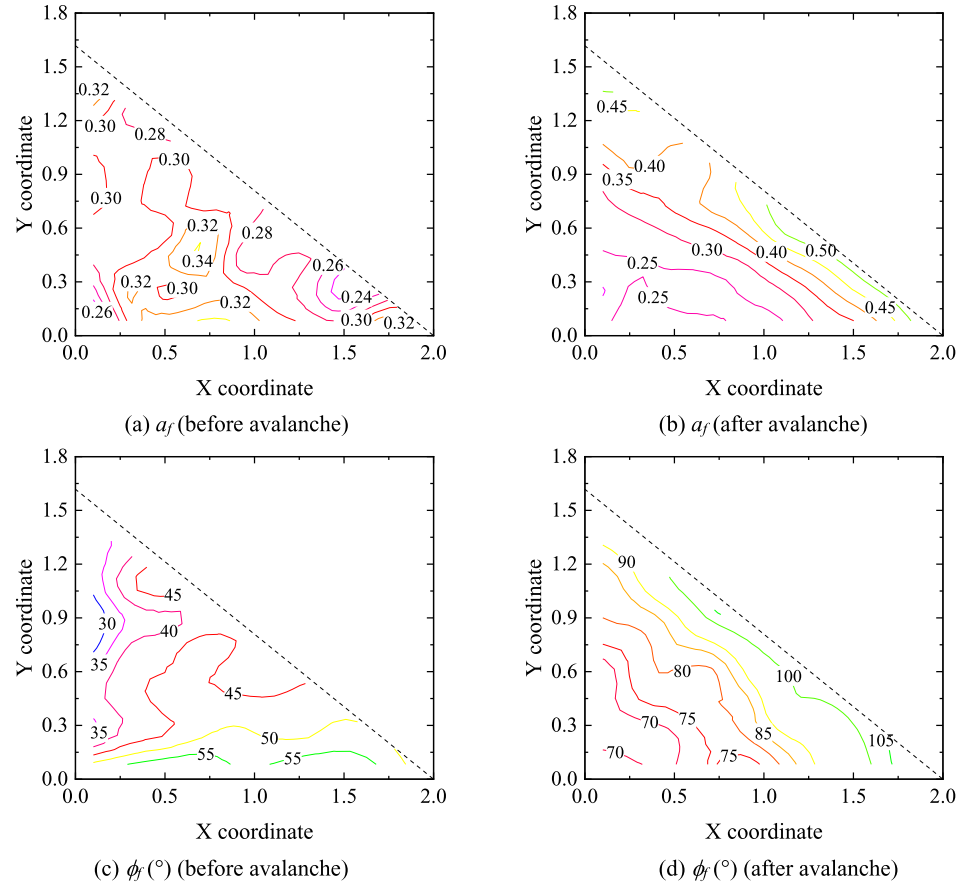

Fig. 19. Comparison of contour maps for the distribution of force anisotropy associated with contact normal forces at the states prior to and after the formation of granular heap ($\theta = 45°$).

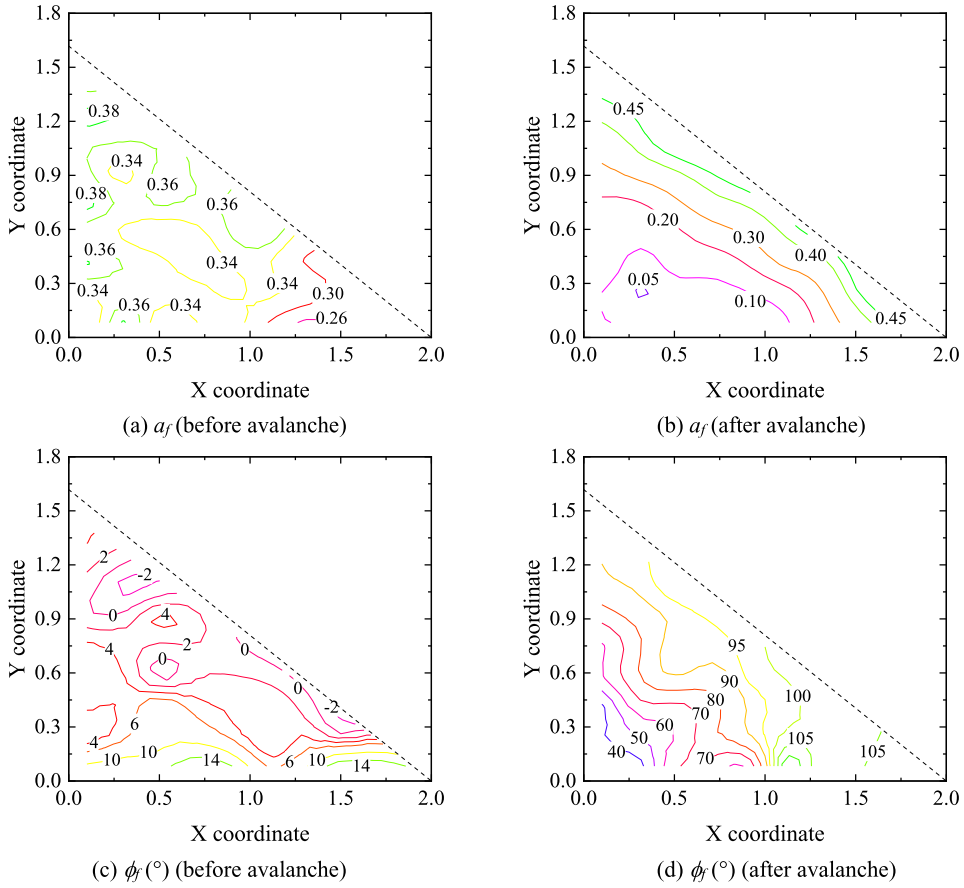

Fig. 20. Comparison of contour maps for the distribution of force anisotropy associated with contact normal forces at the states prior to and after the formation of granular heap ($\theta = 90°$).

repose and the fabric anisotropy, and to bridge the gap between the macroscopic properties and micromechanical responses of granular heaps. It should be mentioned that there exists a superficial zone underneath the slope surface of a granular heap, which suffers from severe disturbance due to granular flows in the avalanche process. We here do the fabric anisotropy analysis of granular heaps, with the exclusion of the zone of strong disturbance since the original microstructures in this zone are almost destructed and the memory of construction history (i.e., the fabric anisotropy induced by particle depositing at various directions) can be easily erased.

By a close examination of Figs. 5, 6 and 11, we find that the angle of repose and the principal anisotropy directions (after avalanche) of ϕ_n and ϕ_p, to some extent, show similar variations with the deposition plane orientation angle θ. It is thus inferred that there may exist a correlation between the angle of repose and the principal anisotropy directions of ϕ_n and ϕ_p. Thus we attempt to establish an expression of angle of repose as a function of ϕ_n and ϕ_p, by introducing a weight factor λ, and this expression is given as

$$\alpha = \lambda\phi_n + (1-\lambda)\phi_p \tag{12}$$

where ϕ_n and ϕ_p are the principal directions of anisotropy relating to the contact unit normal and particle orientation unit

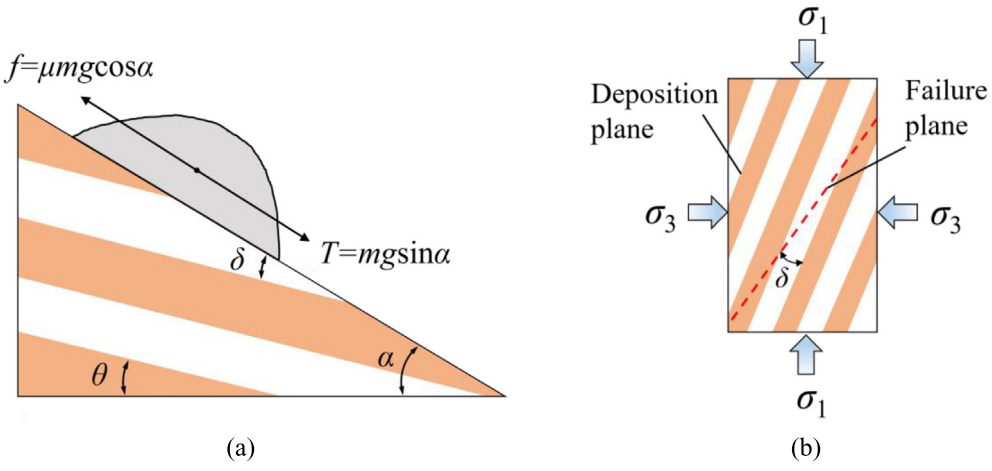

Fig. 21. Schematic illustration of (a) the sliding shear failure of avalanche part under its self weight, and (b) the biaxial shear considering various orientation angles for the deposition plane.

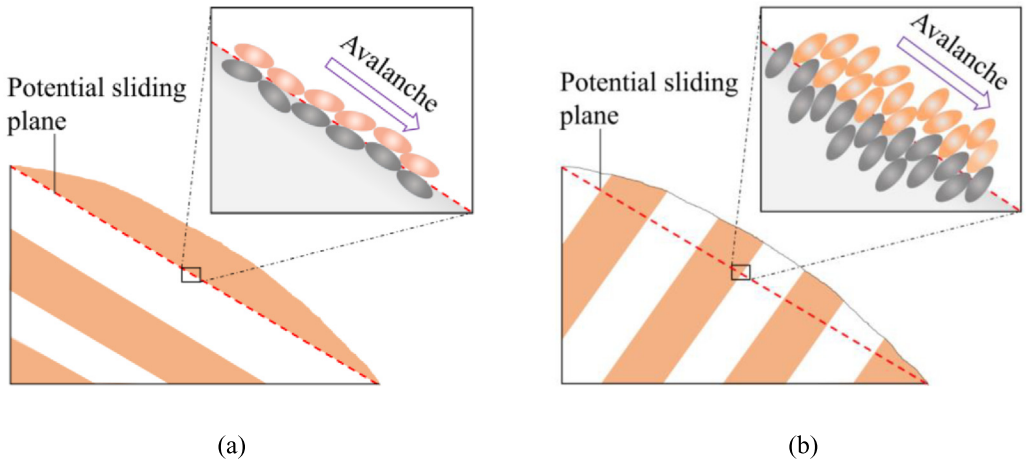

Fig. 22. A microscopic illustration of the effect of fabric on the sliding failure of avalanche part: (a) the deposition plane is parallel to the potential sliding failure plane; (b) the deposition plane deviates from the potential sliding failure plane.

vectors, respectively, and they are determined as the angles of the two principal anisotropy directions relative to the vertical direction.

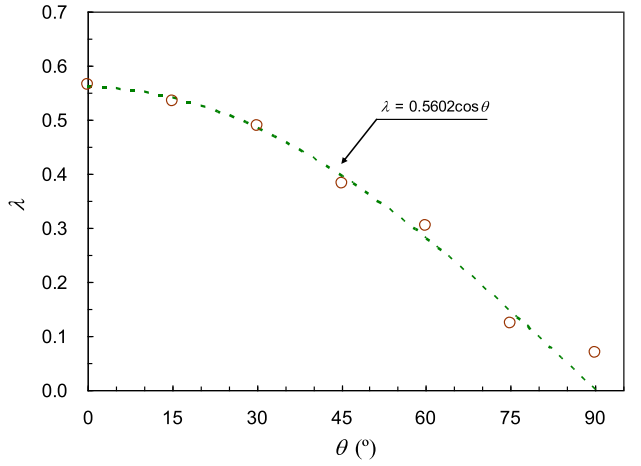

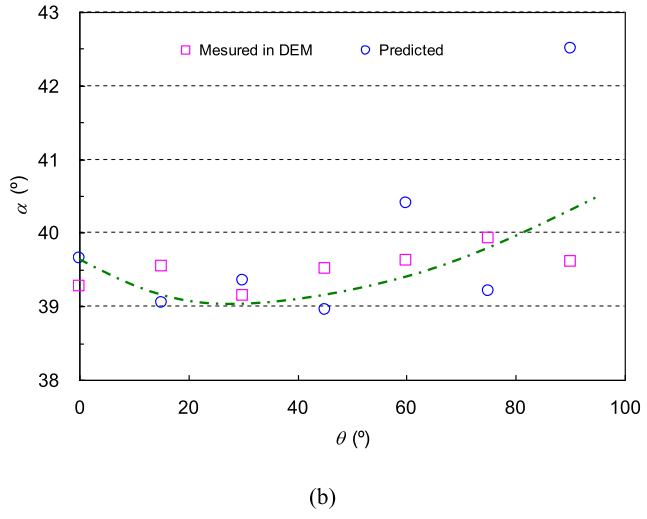

Fig. 23. (a) Correlation of λ with the orientation angle of deposition plane θ, and (b) a comparison of angles of repose measured in the DEM simulations with the values predicted.

With the data of α, ϕ_n and ϕ_p, we back analyze the values of coefficient λ for each deposition plane orientation (θ) case. Since α, ϕ_n and ϕ_p are all dependent on θ, we are strongly motivated to see whether λ is correlated with θ or not. In this connection, we plot λ in Fig. 23a, against the orientation angle θ of deposition plane. As indicated in Fig. 23a, we interestingly identify that the relation of λ with θ can be described by a best fitting cosine curve, the function of which is given to be

$$\lambda = k\cos\theta \tag{13}$$

where the coefficient k is calibrated to be 0.5602 in this study. With the substitution of Eq.(13) into Eq. (12), the angle of repose α is re-expressed as

$$\alpha = \phi_p + 0.5602\cos\theta\left(\phi_n - \phi_p\right) \tag{14}$$

Using Eq. (14), we make a prediction of angle of repose as shown in Fig. 23b, and compare the predicted angle values with those obtained by the DEM simulations. It is seen that the prediction with Eq. (14) can basically capture the variation trend that the angle of repose decreases at first and then rebounds as θ varies from 0° to 90°. Also, the predicted angle values seem not to differ considerably from the measured values from the numerical simulations, except for the case of $\theta = 90°$.

In the industrial processes involved with handing a great amount of discrete particles (e.g. rice grains, powders, sands, pharmaceutical capsules/tablets, etc.), the angle of repose and Hausner ratio are treated as two important indicators of the flowability of granular materials [54–60], the latter of which is defined as the ratio of the tapped bulk density to the aerated (loosely packed) bulk density. The packing density, fabric anisotropy, Hausner ratio, and angle of repose are assumed to be interrelated with each other. A granular assembly at a loosely packed (low packing density) state, which means that the granular assembly may possess a relatively homogeneous or less anisotropic fabric, tends to have a relatively small Hausner ratio or angle of repose. A well packed (high packing density) state is expected to be linked with a fabric of relatively high anisotropy degree, and it is prone to giving a relatively large Hausner ratio or angle of repose. In other words, the degree of fabric anisotropy is positively correlated with the packing density and the values of flowability indicators such as the angle of repose and Hausner ratio.

6. Conclusion

We conducted an experimental and numerical study of the effect of fabric created by the deposition of particles as rainfall at various

directions, on the macro and micro properties of granular heaps. The main findings are summarized as follows:

(a) When the orientation angle θ of deposition plane varies from 0° to 90°, the angle of repose α firstly decreases and then increases, with the minimum value appearing at $\theta = 30° \sim 45°$.

(b) The fabric anisotropy relating to contact orientations before avalanche is featured by an almost constant anisotropy magnitude a_n and a principal anisotropy direction ϕ_n decreasing from about 90° to 0° as θ varies from 0° to 90°. The microstructure reorganizations during the avalanche under the effect of gravity become more and more intense as the angle deviation between the principal anisotropy direction and the vertical gravity direction escalates, making the anisotropy magnitude a_n decrease and the principal anisotropy direction ϕ_n transit toward the vertical direction (90°). At the low θ ($< 45°$) region, the microstructure reorganization gives rise to a kind of "strengthening" effect which makes a_n higher than that before avalanche, and at the high θ region, it contributes to a "crushing" effect which is responsible for a sharp transition of principal anisotropy direction and a minor increase of ϕ_n (after avalanche) beyond the range of $\theta = 45° \sim 75°$.

(c) The relations of the force anisotropy indices a_f and ϕ_f with θ, as well as the involved microscopic mechanism, are basically the same as those revealed for the fabric anisotropy characterized by contact orientations. One distinct difference lies in the absence of the "strengthening" effect of microstructure reorganizations on the force anisotropy magnitude a_f at the low θ region, and this is due probably to the unloading effect arising from the avalanche of surplus granular masses.

(d) The fabric anisotropy associated with particle orientations is characterized by a slight reduction of anisotropy magnitude a_p (before avalanche) and variation of principal anisotropy direction ϕ_p from about 180° to about 90° as θ varies from 0° to 90°. During the formation of granular heaps, the involved microstructure reorganization in terms of particles orientations is not that intense in the low θ ($< 45°$) region, so that both anisotropy magnitude and principal anisotropy direction do not change greatly as compared with their values prior to avalanche. Within the high θ ($\geq 45°$) region, the microstructure reorganization amid the avalanche of redundant particles gets more intense with the further increase of θ, leading to notable transitions in ϕ_p, though a_p does not alter remarkably. The "crushing" effect of the intense microstructure reorganization is present, which causes a marked adjustment of ϕ_p and a minor increase of ϕ_p (after avalanche) following the interim drop at $\theta = 75°$.

(e) The contour maps describing the distribution of various fabric and force anisotropy indices show a similar distribution pattern: the distributions of both anisotropy magnitude and principal direction of anisotropy are in a somewhat uniform mode before avalanche, and they are in a nonuniform fashion owing to the impact of microstructure reorganizations during avalanche; the superficial zone beneath the slope surface of granular heap is mostly influenced, in which the anisotropy magnitude and principal anisotropy direction may both change significantly.

(f) The closer the deposition plane orientation is to the orientation of potential sliding failure plane, the smaller the angle of repose is; the more the deposition plane orientation deviates, the larger the angle of repose is. This is presumably because the interlocking effect along the potential sliding failure plane is comparatively weak if it is almost parallel to the deposition plane, and the work required to overcome the resistances is relatively small when surplus particles avalanche, contributing to a relatively small angle of repose; the interlocking effect is comparatively strong if the orientation deviation between the deposition plane and the potential sliding failure plane gets larger, and there needs to be more work done to overcome the resistances, giving rise to a relatively large angle of repose.

(g) With the introduction of a coefficient λ, a linkage between the angle of repose α and the fabric anisotropy indices of ϕ_n and ϕ_p, has been established. The parameter λ is revealed to be a function of θ, and expressed to be $\lambda = 0.5602\cos\theta$ in current study.

CRediT authorship contribution statement

Bei-Bing Dai: Conceptualization, Methodology, Funding acquisition, Resources, Software, Supervision, Writing – review & editing. **Tian-Qi Li:** Investigation, Software, Data curation, Visualization, Validation, Writing – original draft. **Lin-Jie Deng:** Software, Validation, Data curation. **Jun Yang:** Software, Writing – review & editing. **Wei-Hai Yuan:** Data curation, Writing – review & editing.

Declaration of Competing Interest

The authors declare that they have no known competing financial interests or personal relationships that could have appeared to influence the work reported in this paper.

Acknowledgements

We thank the financial support provided by the National Natural Science Foundation of China (No. 52078507), the Science and Technology Program of Guangzhou City under the grant No. 202002030195 and the Science and Technology Program of Zhuhai City under grant No. ZH22036204200009PWC.

References

[1] I.S. Aranson, L.S. Tsimring, Patterns and collective behavior in granular media: theoretical concepts, Rev. Mod. Phys. 78 (2006) 641–692.
[2] H.P. Jaeger, S.R. Nagel, R.P. Behringer, Granular solids, liquids, and gases, Rev. Mod. Phys. 68 (1996) 1259–1273.
[3] J. Duran, Sands, Powders, and Grains: An Introduction to the Physics of Granular Materials, Springer, New York, 1999.
[4] R. Brockbank, J.M. Huntley, R.C. Ball, Contact force distribution beneath a three-dimensional granular pile, J. Phys. II (7) (1997) 1521–1532.
[5] L. Vanel, D. Howell, D. Clark, R.P. Behringer, E. Clément, Memories in sand: experimental tests of construction history on stress distributions under sandpiles, Phys. Rev. E 60 (1999) R5040–R5043.
[6] N.W. Mueggenburg, H.M. Jaeger, S.R. Nagel, Stress transmission through three-dimensional ordered granular arrays, Phys. Rev. E 66 (2002) 031304.
[7] A.P.F. Atman, P. Brunet, J. Geng, G. Reydellet, P. Claudin, R.P. Behringer, E. Clément, From the stress response function (back) to the sandpile "dip", Eur. Phys. J. E 17 (2005) 93–100.
[8] C. Goldenberg, I. Goldhirsch, Friction enhances elasticity in granular solids, Nature 435 (2005) 188–191.
[9] K. Liffman, M. Nguyen, G. Metcalfe, P. Cleary, Forces in piles of granular materials: An analytic and 3D DEM study, Granul. Matter 3 (2001) 165–176.
[10] Y. Li, Y. Xu, C. Thornton, A comparision of discrete element method simulations and experiments for 'sandpile' composed of spherical particles, Powder Technol. 160 (2005) 219–228.
[11] H.G. Matuttis, Simulation of the pressure distribution under a two-dimensional heap of polygonal particles, Granul. Matter 1 (1998) 83–91.
[12] H.G. Matuttis, S. Luding, H.J. Herrmann, Discrete element simulations of dense packings and heaps made of spherical and non-spherical particles, Powder Technol. 109 (2000) 278–292.
[13] S. Luding, Stress distribution in static two-dimensional granular model media in the absence of friction, Phys. Rev. E 55 (1997) 4720–4729.
[14] Y.Y. Li, D.L. Zhang, B.B. Dai, J. Su, Y. Li, A.T. Yeung, Experimental study on vertical stress distribution underneath granular silos, Powder Technol. 381 (2021) 601–610.
[15] Y.C. Zhou, B.H. Xu, A.B. Yu, P. Zulli, An experimental and numerical study of the angle of repose of coarse spheres, Powder Technol. 125 (1) (2002) 45–54.
[16] J. Lee, H.J. Herrmann, Angle of repose and angle of marginal stability: molecular dynamics of granular particles, J. Phys. A: Math. Gen. 26 (1993) 373–383.
[17] H. Maleki, F. Ebrahimi, E.N. Oskoee, The angle of repose of spherical grains in granular Hele-Shaw cells: a molecular dynamics study, J. Stat. Mech.: Theory Experiment 10 (2008) P04026.
[18] G. McDowell, H. Li, I. Lowndes, The importance of particle shape in discrete-element modelling of particle flow in a chute, Géotechn. Lett. 1 (2011) 59–64.
[19] D.A. Robinson, S.P. Friedman, Observations of the effects of particle shape and particle size distribution on avalanching of granular media, Physica A 311 (2002) 97–110.
[20] B.B. Dai, J. Yang, C.Y. Zhou, Micromechanical origin of angle of repose in granular materials, Granul. Matter 19 (2017) 24.
[21] B.B. Dai, J. Yang, C.Y. Zhou, W. Zhang, Effect of particle shape on the formation of sandpile, Proceedings of the 7th International Conference on Discrete Element Method, Dalian, China 2016, pp. 767–776.

[22] H. Chen, S. Zhao, X. Zhou, DEM investigation of angle of repose for super-ellipsoidal particles, Particuology 50 (2020) 53–66.
[23] J. Alonso, J.P. Hovi, H. Herrmann, Lattice model for the calculation of the angle of repose from microscopic grain properties, Phys. Rev. E 58 (1998) 672–680.
[24] H. Zhao, X. An, D. Gou, B. Zhao, R. Yang, Attenuation of pressure dips underneath piles of spherocylinders, Soft Matter 14 (2018) 4404–4410.
[25] Z.Y. Zhou, R.P. Zou, D. Pinson, A.B. Yu, Angle of repose and stress distribution of sandpiles formed with ellipsoidal particles, Granul. Matter 16 (2014) 695–709.
[26] J. Zhu, Y. Liang, Y. Zhou, The effect of the particle aspect ratio on the pressure at the bottom of sandpiles, Powder Technol. 234 (2013) 37–45.
[27] J.T. Carstensen, P.C. Chan, Relation between particle size and repose angles of powders, Powder Technol. 15 (1976) 129–131.
[28] F. Elekes, E.J.R. Parteli, An expression for the angle of repose of dry cohesive granular materials on Earth and in planetary environments, Proc. Natl. Acad. Sci. 118 (38) (2021) e2107965118.
[29] J. Geng, E. Longhi, R.P. Behringer, D.W. Howell, Memory in 2D heap experiments, Phys. Rev. E 64 (2001) 060301.
[30] J. Horabik, P. Parafiniuk, M. Molenda, Discrete element modelling study of force distribution in a 3D pile of spherical particles, Powder Technol. 312 (2017) 194–203.
[31] C. Zhou, J.Y. Ooi, Numerical investigation of progressive development of granular pile with spherical and non-spherical particles, Mech. Mater. 41 (2009) 707–714.
[32] J. Yang, X.D. Luo, Exploring the relationship between critical state and particle shape for granular materials, J. Mech. Physics Solids 84 (2015) 196–213.
[33] I. Cavarretta, M. Coop, C. O'Sullivan, The influence of particle characteristics on the behavior of coarse grained soils, Géotechnique 60 (6) (2010) 413–423.
[34] B.B. Dai, J. Yang, X.D. Luo, A numerical analysis of the shear behavior of granular soil with fines, Particuology 21 (2015) 160–172.
[35] B.B. Dai, Probing the boundary effect in granular piles, Granul. Matter 20 (2018) 5.
[36] H. Pourtavakoli, E.J.R. Parteli, T. Pöschel, Granular dampers: does particle shape matter? New J. Phys. 18 (2016) 073049.
[37] T. Pöschel, V. Buchholtz, Static friction phenomena in granular materials: Coulomb law versus particle geometry, Phys. Rev. Lett. 71 (1993) 3963–3966.
[38] B. Suhr, K. Six, Simple particle shapes for DEM simulations of railway ballast: influence of shape descriptors on packing behaviour, Granul. Matter 22 (2020) 43.
[39] M. Oda, Fabric tensor and its geometrical meaning, in: M. Oda, K. Iwashita (Eds.), Mechanics of Granular Material: An Introduction, A.A. Balkema, Rotterdam 1999, pp. 27–35.
[40] L. Rothenburg, R.J. Bathurst, Analytical study of induced anisotropy in idealized granular materials, Géotechnique 39 (1989) 601–614.
[41] K. Kanatani, Distribution of directional data and fabric tensors, Int. J. Eng. Sci. 22 (1984) 149–164.
[42] M. Satake, Fabric tensor in granular materials, IUTAM Symposium on Deformation and Failure of Granular Materials, Delft 1982, pp. 63–68.
[43] J. Yang, B.B. Dai, Is the quasi-steady state a real behaviour? A micromechanical perspective, Géotechnique 61 (2) (2011) 175–183.
[44] B.B. Dai, J. Yang, C.Y. Zhou, X.D. Luo, DEM investigation on the effect of sample preparation on the shear behavior of granular soil, Particuology 25 (2016) 111–121.
[45] J.R. Metcalf, Angle of repose and internal friction, Int. J. Rock Mech. Min. Sci. Geomech. Abstr. 3 (2) (1966) 155–161.
[46] Y. Grasselli, H.J. Herrmann, On the angles of dry granular heaps, Physica A 246 (1997) 301–312.
[47] Z. Chik, L.E. Vallejo, Characterization of the angle of repose of binary granular materials, Can. Geotech. J. 42 (2005) 683–692.
[48] J. Frączek, A. Złobecki, J. Zemanek, Assessment of angle of repose of granular plant material using computer image analysis, J. Food Eng. 83 (2007) 17–22.
[49] W. Czarnecki, M. Szumiło, D. Wasik, Influence of size and density of particles on flow properties of granules, Acta Poloniae Pharmaceutica-Drug Res. 66 (5) (2009) 553–561.
[50] P. Fu, Y.F. Dafalias, Study of anisotropic shear strength of granular materials using DEM simulation, Int. J. Numer. Anal. Methods Geomech. 35 (2011) 1098–1126.
[51] K. Miura, S. Miura, S. Toki, Deformation behavior of anisotropic dense sand under principal stress axes rotation, Soils Found. 26 (1986) 36–52.
[52] W. Cao, R. Wang, J.M. Zhang, New strength criterion for sand with cross-anisotropy, Chinese J. Geotechn. Eng. 38 (11) (2016) 2026–2032 (in Chinese).
[53] I. Zuriguel, T. Mullin, The role of particle shape on the stress distribution in a sandpile, Proc. R. Soc. A 464 (2008) 99–116.
[54] D. Geldart, Types of gas fluidization, Powder Technol. 7 (1973) 285–292.
[55] R.O. Grey, J.K. Beddow, On the Hausner ratio and its relationship to some properties of metal powders, Powder Technol. 2 (1969) 323–326.
[56] D. Geldart, Characterization of powder flowability using measurement of angle of repose, China Particuol. 4 (2006) 104–107.
[57] A.W. Jenike, P.J. Elsey, R.H. Woolley, Flow properties of bulk solids, Utah Engineering Station, University of Utah, Bul. 95 (1958).
[58] G. Lumay, F. Boschini, K. Traina, S. Bontempi, J.C. Remy, R. Cloots, N. Vandewalle, Measuring the flowing properties of powders and grains, Powder Technol. 224 (2012) 19–27.
[59] D. McGlinchey, Characterisation of Bulk Solids, Blackwell Publishing, Oxford, 2005.
[60] A.C.Y. Wong, Characterisation of the flowability of glass beads by bulk densities ratio, Chem. Eng. Sci. 55 (2000) 3855–3859.